16. G. Capobianco, P. Venti, and F. Bellucci, *Brit. Corrs. J.*, **25,** 133 (1990).
17. R. G. Kelly and P. J. Moran, *Corros. Sci.*, **30,** 495 (1990).
18. V. Gutmann, *Coordination Chemistry in Non-aqueous Solutions,* Springer-Verlag, Heidelberg (1968).
19. U. Mayer, V. Gutmann, and W. Gerger, *Monath. Chem.*, **106,** 1235 (1975).
20. V. Gutmann and E. Wychera, *Inorg. Nucl. Chem. Lett.*, **2,** 257 (1966).
21. M. Sakakibara, N. Saito, H. Nishihara, and K. Aramakik, *Corros. Sci.*, **34,** 391 (1993).
22. K. Aramaki, M. Hagiwara, and H. Nishihara, *This Journal,* **135,** 1364 (1988).
23. J. O'M. Bockris, D. Drasic, and A. R. Despic, *Electrochim. Acta,* **4,** 325 (1961).
24. Z. Szklarska-Smialowska, in *Proceedings of 7th European Symposium on Corrosion Inhibitors,* Vol. 2, p. 979, Università Degli Studi di Ferrara, Ferrara (1990).
25. Yu. I. Kuznetsov, *Zashch. Metal.*, **20,** 359 (1984).

Electrochemical Studies with Copper-Based Alloys

Open-Circuit Potential Oscillations in Alkaline Media

M. R. F. Hurtado,[a] P. T. A. Sumodjo,[b] and A. V. Benedetti[a]

[a]*Instituto de Quimica da Universidade Estadual Paulista, Araraquara 14800-900, Brazil*
[b]*Instituto de Quimica da Universidade de São Paulo, São Paulo 01498, Brazil*

ABSTRACT

In open-circuit potential measurements of certain Cu-based alloys in NaOH solutions oscillations were observed in Cu-Al and Cu-Ag-Al. Studies with various electrolyte concentrations and rotation speeds of the electrode led to a possible explanation of the phenomenon in terms of Al dissolution altering the main Cu dissolution/passivation process. The accumulation of aluminate ions on the interphase and its transportation to the bulk solution are the main causes of the oscillations.

The copper-based alloys have been developed to produce materials with better properties than pure copper for specific purposes. Particularly, Cu-Al-Ag alloys present shape memory effect and are of special interest in electronics and dentistry. The electrochemical behavior of Cu-Al-Ag alloys is the subject of investigations in our laboratories. The study of microstructural features and the mechanism of anodic oxidation of Cu-Al-Ag alloys in 0.5 mol/liter NaOH have been reported previously.[1,2] The observation of unexpected potential oscillations during the open-circuit potential measurements stimulated our interest in this phenomenon.

Most oscillatory phenomena involving electrochemical systems described in the literature are related to oscillations which arise during the anodic polarization of different metals such as Zn,[3,4] Fe,[5] and Cu.[6-11] Cathodic oscillations also are known.[12,13] With regard to copper electrodissolution, oscillations occurred in deoxygenated chlorate[14] and acidic chloride.[6,8-11] Periodic formation and dissolution of CuO film in the former case, and CuCl film in the latter were recognized as the basis of the phenomenon. Various models to explain this phenomenon have been proposed.[8,14-16] However, copper oscillations in neutral chloride or in alkaline media have never been reported, while anodic and cathodic oscillations are well known in the literature. Open-circuit potential oscillations are unusual.[5] One which has been well described in the literature is related to the Fe/H_2SO_4 electrode in the presence of BrO_3^- ions.[5] There is a natural oscillatory phenomenon observed during open-circuit potential measurements of a Cu-Ag-Al alloy in NaOH solutions.

Experimental

The alloy studied here was prepared from 99.99% Cu, Al, and Ag according to the procedure described previously.[17] As determined by spectrographic analysis its composition was the following: Ag, 49.9%; Cu, 45.7%; and Al, 3.9%. The material was annealed at 830°C for 140 h and cooled slowly. After which the alloy presents two phases: α_1 (a solid solution of Al and Ag in Cu) and α_2 consisting of a solid solution of Al and Cu in Ag, as observed via scanning electron microscope (SEM) and energy-dispersive x-ray (EDX)[1] which has been described in the literature.[18] Working electrodes were then made by embedding alloy cylinders in Araldite holders to expose a disk with a diameter of 4.0 mm to the solution. Electrode potentials were measured with respect to a reversible hydrogen electrode in the same solution (hess), connected to the cell via a Luggin capillary. All the potentials given here are referred to this electrode. The aerated NaOH electrolyte with various concentrations, was prepared from tridistilled water and Merck p.a. NaOH. The instrumentation consisted of a PAR 273 (Princeton Applied Research) potentiostat-galvanostat, equipped with computer control data acquisition.

Prior to each potential-time measurement the electrode was polished mechanically with different grades of emery paper and diamond paste and then degreased with acetone to remove the smut, after which the electrode was rinsed in acetone and water and immersed in the cell.

Experiments with the pure Cu and Ag metals, Cu-3.9Al, Ag-4Al, Cu-Ag, and Ag-Cu alloys also were carried out. The Cu-Al alloy consists of a solid solution while the Ag-Al system shows a solid solution of Al dissolved in Ag. The Ag_3Al μ-phase is not well established at room temperature for this composition.[18,19] Cu-Ag and Ag-Cu present two phases since the solubility of one metal in the other is very low at room temperature.[18]

Results

Figure 1a shows a typical open-circuit *E vs. t* curve obtained for the Cu-Ag-Al alloy electrode in aerated 0.5 mol/liter NaOH. Immediately after the electrode immersion into the solution, the potential rises rapidly from 0.56 ± 0.02 to 0.73 V, followed by a smooth rise, finally reaching 0.77 V. The potential remains essentially constant for approximately 750 s, and afterward undergoes an abrupt drop to 0.56 V. After a slight rise to 0.58 V, it increases rapidly to 0.73 V, restarting the cycle (Fig. 1b). Potential oscillations cease after 45,000 s, with the potential reaching a steady value of 0.89 V after approximately 60,000 s. The oscillations described do not occur when the electrode is dipped in deaerated electrolyte, and the immersion potential remains practically constant (Fig. 1c).

To understand the phenomenon better, the influence of variables such as electrolyte concentration, agitation of the solution, and composition of the electrode were studied.

The effect of the NaOH concentration on the oscillations was studied in the [NaOH] range from 0.01 to 0.3 mol/liter

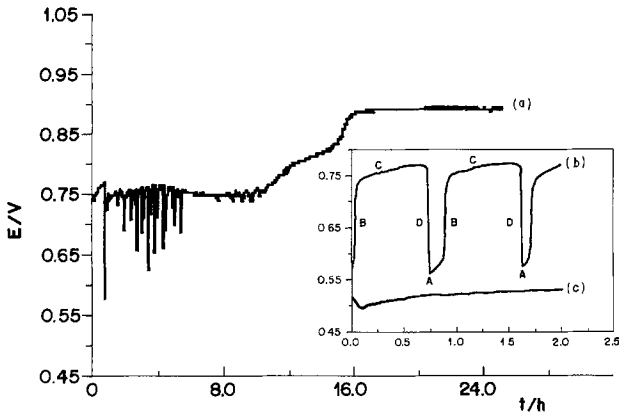

Fig. 1. Open-circuit potential-time curve for an annealed Cu-Ag-Al alloy electrode at 25°C; (a) in aerated 0.5 mol/liter NaOH; (b) in aerated 0.5*M* NaOH with extended *x* axis to detail the oscillations; (c) in deaerated 0.5 mol/liter NaOH.

at constant ionic strength of 0.5 mol/liter by addition of $NaClO_4$. The oscillations are similar to those already observed in Fig. 1b. The main difference is an increase in the duration of the oscillations with the electrolyte concentration (Fig. 2).

The study of the effect of agitation revealed that there is a threshold value in rotation rate, above which potential oscillations were not observed. As can be seen in Fig. 3a, rotation rates greater than 3000 rpm hamper the oscillations. Figure 3b shows the result of the curve obtained for an open-circuit potential measurement with varying rotation rates; the oscillations cease at a lower rotation rate of 45 rpm due to time restriction.

The influence of the electrode material on the oscillations was studied for pure Cu and Ag electrodes, and for the following alloy electrodes: Cu-Al, Ag-Al, and Cu-Ag. The former two alloy electrodes contain the same quantity of aluminum as in the ternary alloy and all were submitted to the same heat-treatment. Figures 4a and b show the resulting *E/t* curves for the pure metal electrodes, copper and silver, respectively. The immersion potential observed for the Cu electrode is 0.77 V, and this value is maintained for *ca.* 15,000 s. The potential then goes up to 0.86 V, remaining constant until the end of the experiment. When a Ag electrode is dipped into the electrolyte, the potential shows a

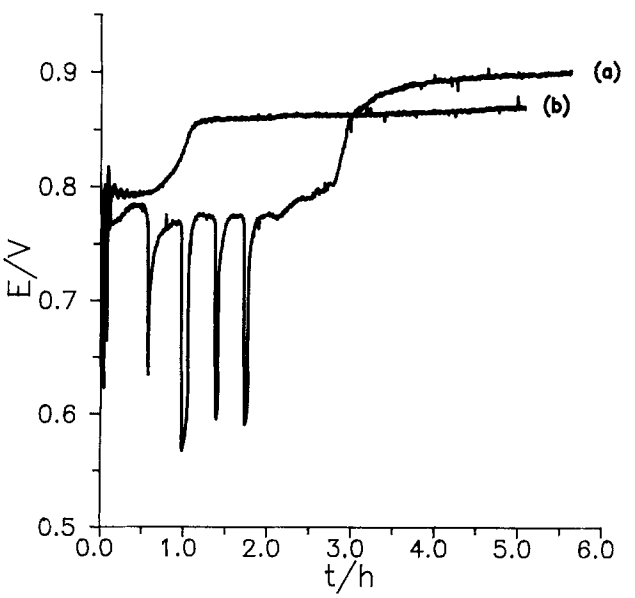

Fig. 2. Potential-time curves for the Cu-Ag-Al alloy in aerated NaOH solutions with different concentrations (mol/liter) and constant ionic strength equal to 0.5 mol/liter [$NaClO_4$]; *T* = 25°C; (a) 0.3 and (b) 0.075.

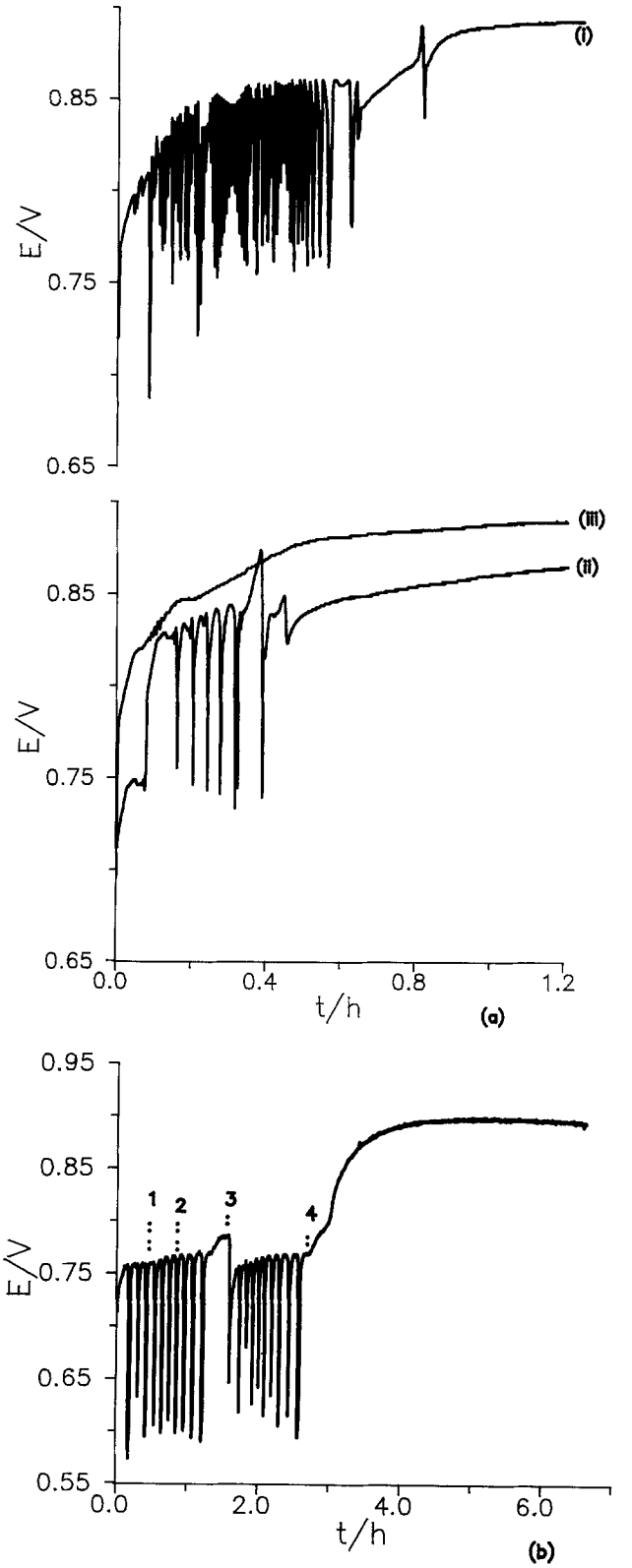

Fig. 3. Potential-time curve for a rotating Cu-Ag-Al alloy electrode obtained (a) for different rotation rates (rpm): (*i*) 1500; (*ii*) 2500, and (*iii*) 3000; (b) with varying rotating speeds, in 0.5 mol/liter NaOH. Initial rotating rate, 20 rpm. Numbers in the figure denote new rpm; (1) 25; (2) 35; (3) 40; and (4) 45.

slight decrease from the immersion value followed by a very slow rise. In both situations no oscillations are observed, as has already been pointed out in the literature.[20-23] In the same pattern, oscillations were not observed with the Ag-Al and the Cu-Ag alloys. Nevertheless, the Cu-Al alloy does exhibit oscillations (Fig. 4c). The immersion potential is 0.52 V and during the first 15,000 s oscillations are clearly

noted. After a period of *ca.* 40,000 s it becomes constant around 0.89 V. No experiments were performed with an aluminum electrode as it is well known that in alkaline media it undergoes chemical dissolution.

Discussion

The findings from these experiments indicate that the observed potential oscillations during open-circuit measurements of Cu-Ag-Al alloy in NaOH solutions depend on the dissolved oxygen, the electrolyte concentration, and the rotation speed of the electrode. Concerning the solid phase, copper and aluminum are responsible for the phenomenon and, possibly Ag takes no part in it.

In a typical experiment using 0.5 mol/liter NaOH, in one cycle, the following potential variation can be seen (Fig. 1b):

step A—smooth increase from *ca.* 0.56 to 0.58 V;
step B—instantaneous rise from *ca.* 0.58 to 0.73 V;
step C—smooth increase from 0.73 to 0.77 V;
step D—instantaneous decay from 0.77 to *ca.* 0.56 V

with a decrease of the oscillation period and a slight shift of the cathodic limit, around 20 mV, to more positive values in each subsequent cycle.

Examination of the Pourbaix diagram for aluminum reveals that for a pH corresponding to a 0.5 mol/liter NaOH solution, Al undergoes a rapid dissolution to form the aluminate ion according to the following equations[24]

$$2Al + 4H_2O \rightarrow 2AlO_2^- + 8H^+ + 6e^- \quad [1]$$

$$1\ 1/2\ O_2 + 3H_2O + 6e^- \rightarrow 6\ OH^- \quad [2]$$

$$2Al + H_2O + 1\ 1/2\ O_2 \rightarrow 2AlO_2^- + 2H^+ \quad [3]$$

causing a decrease in the pH value at the interface and therefore, neutralization of the H^+ ions must occur

$$H^+ + OH^- \rightarrow H_2O \text{ (at the interface)} \quad [4]$$

It is well known that copper is oxidized to form cuprous oxide in solutions containing dissolved oxygen.[25] As has been described in the literature, this oxidation to form Cu_2O proceeds via a two-step mechanism involving the $Cu^+_{surface}$ species.[21] In open circuit the reactions involved are

$$2Cu \rightarrow 2Cu^+_{surface} + 2e^- \quad [5]$$

$$1/2\ O_2 + H_2O + 2e^- \rightarrow 2\ OH^- \quad [6]$$

$$2Cu + 1/2\ O_2 + H_2O \rightarrow 2Cu^+_{surface} + 2\ OH^- \quad [7]$$

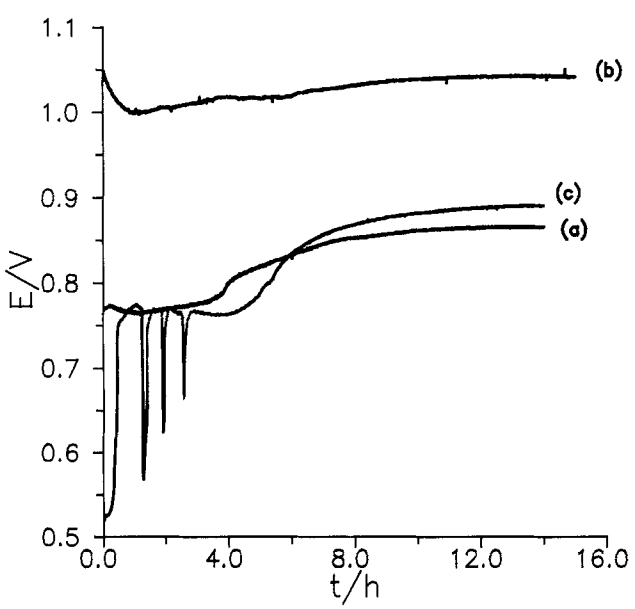

Fig. 4. Different electrode material potential-time curves in aerated 0.5 mol/liter NaOH: (a) pure Cu; (b) pure Ag; and (c) Cu-Al alloy.

$$2Cu^+_{surface} + 2\ OH^- \rightarrow Cu_2O(s) + H_2O \quad [8]$$

The cuprous oxide formed in alkaline medium, dissolves to form complexing species such as $Cu_2O_2H^-$ and $Cu_2O_2^{2-}$, according to Eq. 9

$$Cu_2O(s) + OH^-(aq) \rightleftarrows Cu_2O_2H^-(aq) \quad [9a]$$

$$Cu_2O_2H^-(aq) + OH^-(aq) \rightleftarrows Cu_2O_2^{2-} + H_2O \quad [9b]$$

as detected by Arvia *et al.*[26] and Miller[27] with the rotating ring-disk electrode (RRDE) technique. The Cu(I) species are unstable, and in the presence of O_2 undergo further oxidation to form Cu(II) species. The following considerations are presented to explain our observations.

The initial potential rise, step A, (Fig. 1b) can be explained admitting that, as the electrode is immersed into the solution, aluminum and copper begin to oxidize according to Eq. 3 and 7. Since aluminum is the minor alloy component, and oxidation ceases when OH-ions can no longer reach the Al atoms, *i.e.*, as Al dissolves preferentially,[1] oxidation occurs with the formation of micropores, impeding further interaction with the OH^- ions. Both reactions happen with O_2 consumption, pH increase at the interface due to the formation of H^+ ions and their neutralization, and OH^- production, leading to the development of different charged species, AlO_2^- and Cu(I). The accumulation of these two different charged species, plus the slow diffusion of the aluminate ion to the bulk solution, account for the slow potential increase. When the interface properties are no longer influenced by the presence of the aluminate ions, *i.e.*, the Cu/Cu^+ ions system governs the establishment of the electrical potential difference across the interface, the potential abruptly increases to a value around 0.73 V, step B.

In step C, copper continues to oxidize to form the Cu(I) species which, in turn, can react with the hydroxyl ions to form a layer of cuprous oxide, Eq. 8, making the potential rise slowly from 0.73 to 0.77 V, in approximately 2600 s. This can be deduced by the potential value reached at the end of step B, *ca.* 0.73 V, a potential attributed to the formation of the Cu(I) species.[2] At step C, there may be an increase of the $Cu^+_{surface}$ species due to further copper oxidation (Eq. 7). This provokes a diffusion of OH^- ions from the bulk solution to restore the charge balance. At a certain moment the Cu_2O solubility product is attained at the interface and cuprous oxide precipitates on the electrode surface. Figure 5 illustrates the micrograph of the electrode surface *ca.* 20 min after the beginning of step C and shows a surface partially covered by a gel. In the presence of excess hydroxyl ions, Cu_2O can solubilize according to Eq. 9 and the soluble Cu(I) species in the presence of oxygen can undergo further oxidation

$$Cu_2O_2H^-(aq) + 1/2\ O_2 + 2H_2O \rightarrow 2Cu^{2+}(aq) + 5\ OH^- \quad [10a]$$

$$Cu_2O_2^{2-}(aq) + 1/2\ O_2 + 3H_2O \rightarrow 2Cu^{2+}(aq) + 6\ OH^- \quad [10b]$$

During this long step, $Cu^+_{surface}$ ions accumulate on the surface, Cu_2O is formed and dissolved, which causes further metallic copper oxidation. This oxidation proceeds up to a certain instant when aluminum atoms are again exposed to the electrolyte allowing oxidation. Thus, at a certain instant, a bare surface similar to the one found at the beginning of the experiment is exposed to the electrolyte dropping the potential to a value approximately equal to the immersion potential which explains step D.

Interrupting the experiment when the potential has reached its lower value, a cleaner surface is observed (Fig. 6) in comparison with the surface shown in Fig. 5. Aluminum dissolution proceeds forming new micropores, causing an increase of AlO_2^- ions concentration at the interphase, and copper oxidation, reinitiating step A of the cycle.

As each cycle is completed, the next lower potential value in step A becomes slightly more positive than the former. This fact is due to the increase in the concentration

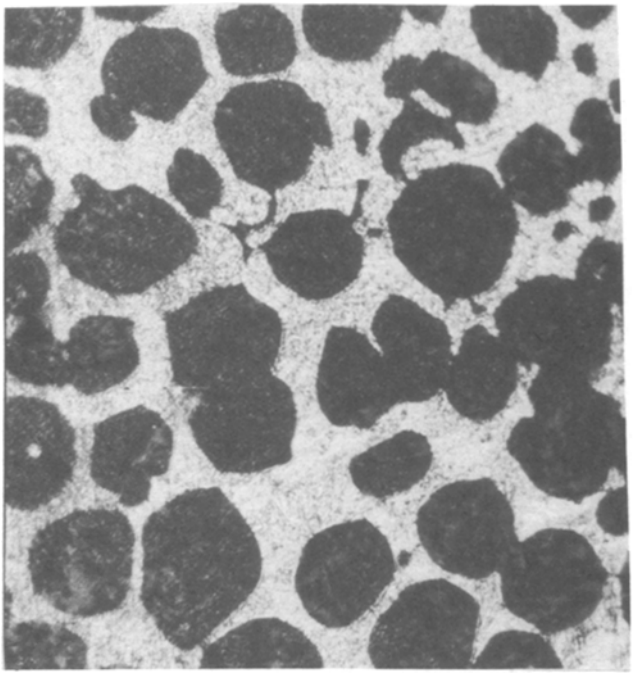

Fig. 5. Micrograph of the Cu-Ag-Al alloy surface after the attainment of an open-circuit potential of 0.77 V/hess in aerated 0.5 mol/liter NaOH; 250× magnification.

of the Cu^{2+} ions with time. This increase in $[Cu^{2+}]$ causes a decrease in the dissolution rate of the film of cuprous oxide. Consequently, at each cycle, the free available surface area undergoing chemical dissolution of the metal diminishes which may lead to a complete inhibition of the oscillations when a certain critical $[Cu^{2+}]$ is reached. The addition of $CuSO_4$ to the solution in a concentration equal or greater than its solubility causes no oscillations. The subsequent increase observed in the potential can be attributed to reactions 10 and 11

$$Cu_2O + 2H_2O + 1/2\ O_2 \rightarrow 2Cu(OH)_2 \qquad [11]$$

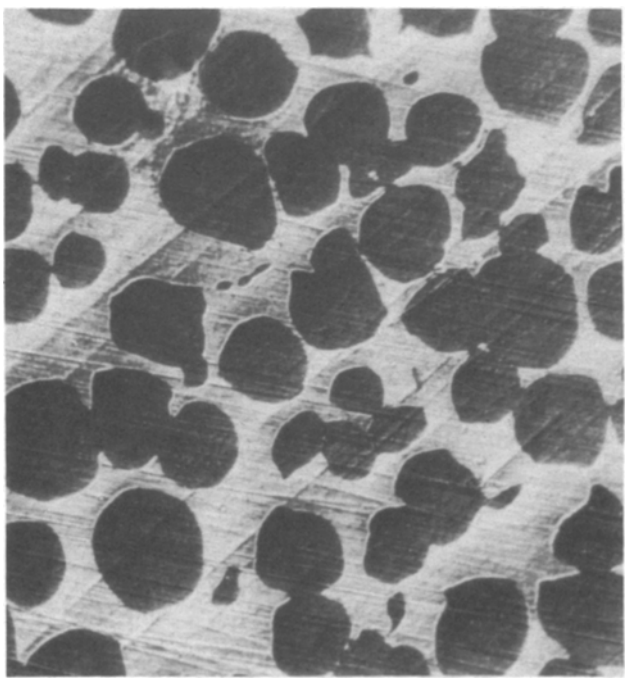

Fig. 6. Micrograph of the Cu-Ag-Al alloy surface after the attainment of an open-circuit potential of 0.56 V/hess in aerated 0.5 mol/liter NaOH; 250× magnification.

The value of 0.89 V is attributed to the formation of Cu(II) species.[2,26,27] Cupric hydroxide can be dissolved in alkaline solutions to form the CuO_2H^- and CuO_2^{2-} species[26,27] and also can pass through an aging process to form CuO. It is a well-established fact that copper in alkaline solutions yields $Cu|Cu_2O|CuO|Cu(OH)_2|OH^-$ type multiplex film.[26]

The conclusion, therefore, is that the oscillatory phenomenon observed is due to the presence of aluminum on the electrode surface since pure copper presents no oscillations (Fig. 4a). In this case, reactions involving the formation and dissolution of Cu_2O and formation of $Cu^{2+}(aq)$, (Eq. 7-10) account for the first potential plateau observed at *ca.* 0.77 V. The increase in Cu^{2+} concentration causes the potential to rise. As $[Cu^{2+}]$ at the surface reaches a value corresponding to its solubility, $Cu(OH)_2$ precipitates according to Eq. 12

$$Cu^{2+}(aq) + 2\ OH^-(aq) \rightarrow Cu(OH)_2(s) \qquad [12]$$

resulting in the second potential plateau observed at *ca.* 0.89 V.[2,26,27]

The results show that in the oxygen-free electrolyte there are no oscillations and the potential reaches a constant value at *ca.* 0.52 V. In this case only Al dissolution takes place (Eq. 1) since Cu oxidation should raise the potential to a more positive value. The slight increase in the potential noted in Fig. 1c possibly could be due to the solubilization of a small quantity of oxygen during the long experimental period.

As the electrolyte concentration is diminished there is a reduction in the time of oscillations (Fig. 1a and 2). The $[OH^-]$ decrease leads to a decline in the cuprous oxide dissolution rate (step C) making Al atoms less accessible to the OH^- ions.

The removal rate of the aluminate ions from the surface accounts for the influence of the electrode rotation. When the solution is stirred, AlO_2^- transport to the bulk solution is enhanced and therefore the observed oscillation time can be diminished as the stirring is more effective. Hence, oscillation inhibition can be achieved depending on the electrode rotation rate.

Other binary alloys such as Cu-Ag, Ag-Cu, and Ag-Al, do not present oscillations in 0.5*M* NaOH, since Ag is stable in this medium and the formation of copper oxides for the first two materials account for the potential/time curves. Considering that aluminum is soluble in 0.5*M* NaOH, the potential/time profile for Ag-Al alloy is due to aluminum oxidation.

Conclusion

Copper dissolution and oxide formation is the main process occurring during open-circuit measurements of Cu-Al and Cu-Ag-Al alloys in NaOH solutions. The potential oscillations in aerated solutions are due basically to fast Al dissolution and the slow aluminate ion transport from the surface which alter the main process.

A decrease in OH^- concentration causes a decline in the cuprous oxide dissolution rate resulting in a decrease in the duration of the oscillations.

When the solution is stirred, the removal of aluminate ions from the surface is enhanced which can completely hamper the oscillation depending on the rotation rate.

Acknowledgment

Financial support from the Conselho Nacional de Desenvolvimento Científico e Tecnológico, CNPq, and Fundação de Amparo à Pesquisa do Estado de São Paulo, FAPESP, Brazil, is gratefully acknowledged. The authors are very grateful to Dr. A. T. Adorno for helpful suggestions and technical assistance. They express their appreciation to Dr. W. Li for her reading of the manuscript and for her valuable comments.

Manuscript submitted July 6, 1992; revised manuscript received Feb. 8, 1993.

FAPESP assisted in meeting the publication costs of this article.

REFERENCES

1. P. L. Cabot, F. A. Centellas, J. A. Garrido, P. T. A. Sumodjo, A. V. Benedetti, and R. Z. Nakazato, *J. Appl. Electrochem.*, **21,** 446 (1991).
2. A. V. Benedetti, R. Z. Nakazato, P. T. A. Sumodjo, P. L. Cabot, F. A. Centellas, and J. A. Garrido, *Electrochim. Acta,* **36,** 1094 (1991).
3. M. C. H. McKubre and D. D. MacDonald, *This Journal,* **129,** 524 (1981).
4. R. W. Powers and M. W. Breiter, *ibid.,* **116,** 719 (1969).
5. F. D'Alba, S. Lorenzo, and C. Lucarine, *Electrochim. Acta,* **34,** 709 (1989); *J. Electroanal. Chem. Interfacial Electrochem.,* **271,** 49 (1989).
6. H. P. Lee and K. Nobe, *This Journal,* **132,** 1031 (1983).
7. F. N. Albahadily and M. Schell, *J. Chem. Phys.,* **88,** 4321 (1988).
8. H. P. Lee and K. Nobe, *This Journal,* **132,** 2159 (1983).
9. M. R. Basset and J. L. Hudson, *J. Phys. Chem.,* **93,** 2731 (1989).
10. M. R. Basset and J. L. Hudson, *This Journal,* **137,** 922 (1990).
11. M. R. Basset and J. L. Hudson, *ibid.,* **137,** 1815 (1990).
12. J. St. Pierre and D. L. Piron, *ibid.,* **134,** 1689 (1987).
13. J. St. Pierre and D. L. Piron, *ibid.,* **137,** 2491 (1990).
14. J. F. Cooper, R. H. Muller, and C. W. Tobias, *ibid.,* **127,** 1733 (1980).
15. H. Degn, *Trans. Faraday Soc.,* **64,** 1348 (1968).
16. M. R. Basset and J. L. Hudson, *This Journal,* **137,** 1815 (1990).
17. A. T. Adorno, M. Cilense, and W. Garlipp, *J. Mater. Sci.,* **8,** 281 (1989).
18. *Metals Reference Book,* 5th ed., C. J. Smithells, Editor, Butterworth, London (1976).
19. A. G. Dirks and H. H. Brongersma, *This Journal,* **127,** 2043 (1980).
20. L. D. Burke, J. G. Ahern, and T. G. Ryan, *ibid.,* **137,** 553 (1990).
21. L. D. Burke and T. G. Ryan, *ibid.,* **137,** 1358 (1990).
22. J. M. M. Drood and F. Huisman, *J. Electroanal. Chem. Interfacial Electrochem.,* **115,** 211 (1980).
23. M. Lopez Teijelo, J. R. Vilche, and A. J. Arvia, *ibid.,* **131,** 331 (1982); *J. Appl. Electrochem.,* **18,** 691 (1988).
24. M. Pourbaix, *Atlas of Electrochemical Equilibria in Aqueous Solutions,* pp. 168-175, Cebelcor, Houston, TX (1974).
25. U. Bertocci and D. R. Turner, in *Encyclopedia of Electrochemistry of the Elements,* Vol. II, A. J. Bard, Editor, Marcel Dekker, New York (1974).
26. J. G. Becerra, R. C. Salvarezza, and A. J. Arvia, *Electrochim. Acta,* **33,** 613 (1988).
27. B. Miller, *This Journal,* **116,** 1675 (1969).

Potential pH Diagrams for Sulfur and Oxygen Adsorbed on Nickel in Water at 25 and 300°C

Philippe Marcus and Elie Protopopoff

Laboratoire de Physico-Chimie des Surfaces-CNRS-URA 425,
Ecole Nationale Supérieure de Chimie de Paris, 75231 Paris Cedex 05, France

ABSTRACT

The principle of equilibrium potential-pH diagrams for two-dimensional species adsorbed on metals[3] is applied to the case of sulfur and oxygen adsorbed on nickel in water. Standard Gibbs energies of formation for sulfur and oxygen adsorbed on nickel are calculated from literature thermodynamic data for chemisorption from the gas phase. The E-pH relations associated with the equilibria between water, the dissolved sulfur species, and adsorbed sulfur and oxygen are given at 25 and 300°C. The corresponding E-pH diagrams are drawn for two sulfur activities (10^{-4} and 10^{-6}) and superimposed on the usual Pourbaix diagrams for the S-Ni-H_2O system. Formation of adsorbed sulfur monolayers on the metal surface is predicted in E-pH domains where the usual diagrams do not predict the stability of a nickel sulfide. The E-pH diagrams for species adsorbed on metals allow one to make new predictions of the corrosion risk for metals in sulfur-containing aqueous environments.

The only solid compounds taken into account in the usual equilibrium potential-pH diagrams (Pourbaix diagrams) have been three-dimensional compounds.[1] In previous papers,[2,3] we have shown how the principle of potential-pH diagrams may be extended to take into account two-dimensional phases of elements adsorbed on metals (these elements may be *e.g.,* H, O, N, or S). The prediction of stability domains of adsorbed monolayers is of some importance as the presence of an adsorbed monolayer on the surface can markedly change the reactivity of a metal. In corrosion, a monolayer of sulfur adsorbed on Ni or Ni-Fe alloys enhances the anodic dissolution and hinders the formation of the passive film, drastically affecting the corrosion resistance of the metal or alloy.[4,5] In our previous papers we have constructed the E-pH diagrams for sulfur adsorbed on platinum[2] and iron[3] in water, at 25°C [2,3] and at 300°C.[3] The aim of the present work is to construct the E-pH diagrams for sulfur and oxygen adsorbed on nickel in water containing $H_2S_{(aq)}$, HS^-, HSO_4^-, and SO_4^{2-}. The principle of the calculation is given briefly. Then the standard Gibbs energies of formation for sulfur and oxygen adsorbed on the surface of nickel are calculated at 25 and 300°C from literature thermodynamic data for chemisorption from the gas phase. The E-pH relations associated with the various equilibria between water, the dissolved sulfur species and adsorbed sulfur and oxygen are established. Then diagrams are constructed for two activities of dissolved sulfur species.

Principle of E-pH Diagrams for Adsorbed Species

The principle of calculation of the E-pH relations involving adsorbed species has been given previously.[3] The bases of the calculation are given here:

1. An element A, (*e.g.,* O, S, N, or H) adsorbs on a metal M as an atomic layer, with zero valency [denoted A_{ads} (M)]. The adsorption of A from a species dissolved in aqueous medium may be an electro-oxidation or an electroreduction reaction, depending on the oxidation number (valence state) of A in the dissolved species.
2. The adsorption of the element on the surface of the metal occurs in aqueous medium by replacement of adsorbed water molecules [H_2O_{ads} (M)].
3. A Langmuir model is considered for adsorption: it is assumed that water, oxygen, and sulfur adsorb competitively on the same surface sites and that there are no interactions between adsorbed species.

Under these conditions the chemical potentials for sulfur, oxygen, and water in the phase adsorbed on a metal M can be expressed as follows

$$\mu_{S_{ads(M)}} = \mu^{\circ}_{S_{ads(M)}} + RT \ln 2\theta_s \quad [1]$$